

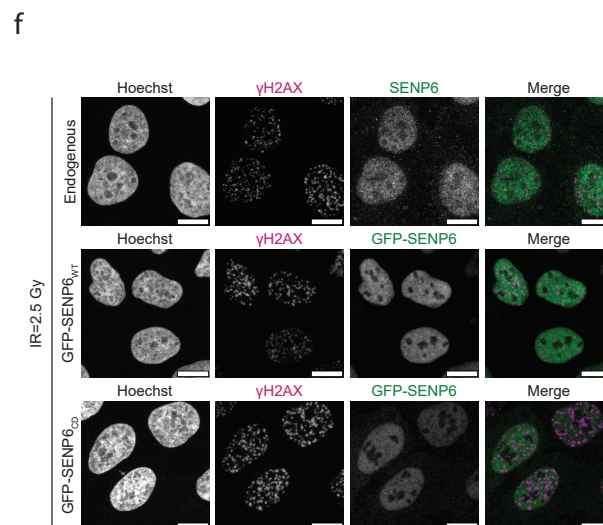
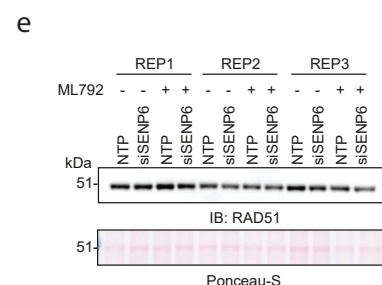
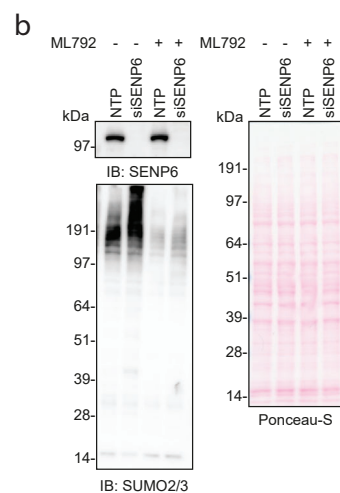
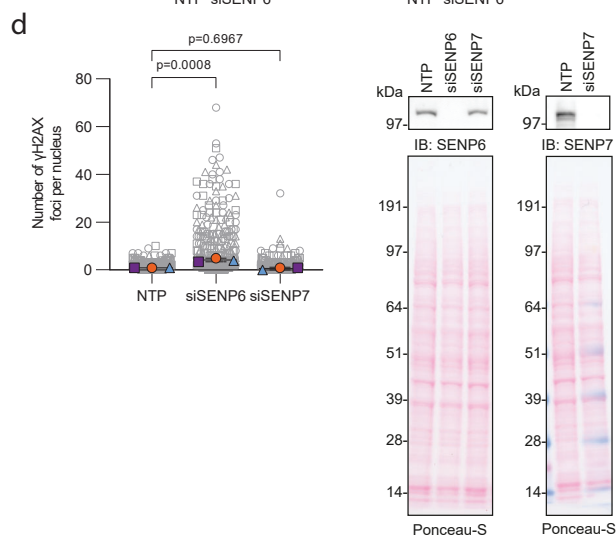
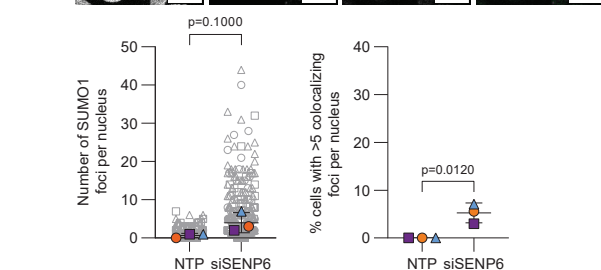
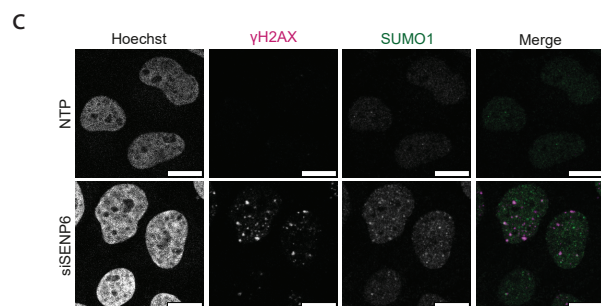
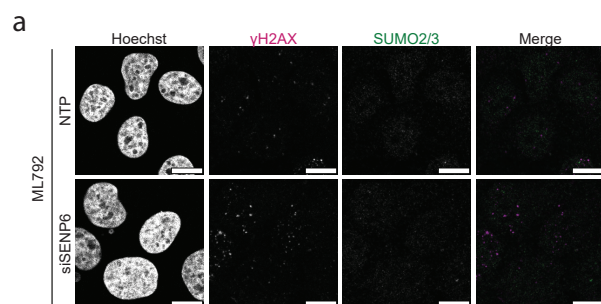
# SENP6 regulates localization and nuclear condensation of DNA damage response proteins by group deSUMOylation

Laura A. Claessens<sup>1</sup>, Matty Verlaan-de Vries<sup>1</sup>, Ilona J. de Graaf<sup>1</sup>, Alfred C.O. Vertegaal<sup>1\*</sup>

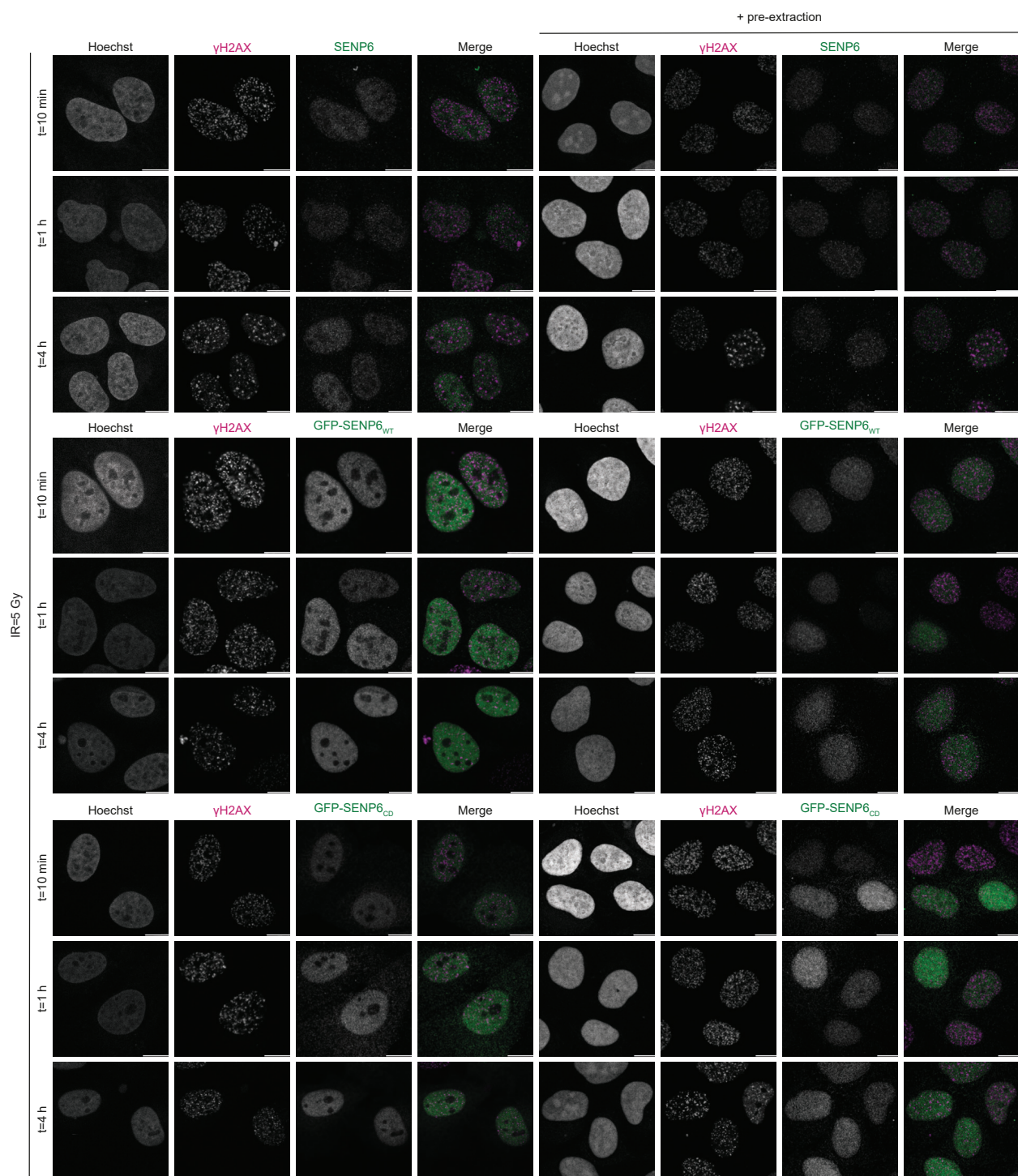
1. Cell and Chemical Biology, Leiden University Medical Centre, Leiden, The Netherlands.

\* Correspondence: vertegaal@lumc.nl

**Supplement**

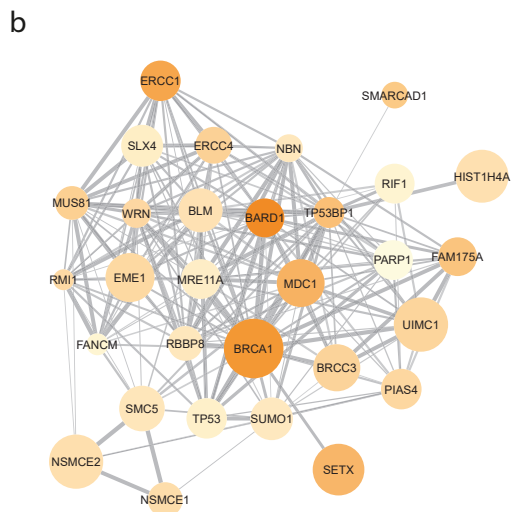
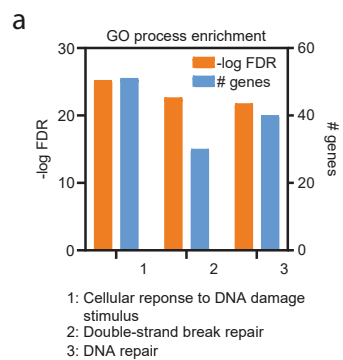


**Supplementary Fig 1. DNA damage observed after SENP6 knockdown is induced through excessive SUMOylation.** **a** Representative images corresponding to Fig. 1b, n=3. **b** Lysates from cells corresponding to Fig. 1b-e were immunoblotted for SENP6 and SUMO2/3, n=3. Equal loading was verified by Ponceau-S staining. A representative blot is shown. **c** U2OS were treated with SENP6 (siSENP6) or nontargeting (NTP) siRNAs for 72 h and analyzed by immunofluorescence staining for  $\gamma$ H2AX (magenta) and SUMO1 (green), n=3. Left graph: quantification of number of SUMO1 foci per nucleus. Data are shown as pooled cells (from left, n=309,305 cells) (grey), superimposed by the median number of foci per experiment (orange, blue and purple). Right graph: quantification of percentage of cells >5 colocalizing foci per nucleus. Significance was determined with a two-sided unpaired t-test. Cells were also analyzed by immunoblotting for SENP6, n=3. Equal loading was verified by ponceau-S staining. A representative blot is shown. **d** U2OS were treated with SENP6 siRNAs (siSENP6), SENP7 siRNAs (siSENP7) or nontargeting siRNAs (NTP) for 72 h and analyzed by immunofluorescence staining for  $\gamma$ H2AX, n=3. Quantification of number of  $\gamma$ H2AX foci per nucleus. Data are shown as pooled cells (from left, n=317,327,366 cells) (grey), superimposed by the median number of foci per experiment (orange, blue and purple). Significance was determined by two-sided one-way ANOVA with Dunnett's multiple comparison test. Cells were also analyzed by immunoblotting for SENP6 and SENP7, n=3. Equal loading was verified by ponceau-S staining. Representative blots are shown. **c,d** Error bars in graphs represent mean  $\pm$ SD. Independent experiments are visualized by unique symbols. **e** Lysates from cells in **(b)** were immunoblotted for RAD51, n=3. Equal loading was verified by Ponceau-S staining. **f** Top panel: U2OS were treated with ionizing radiation (IR) and analyzed by immunofluorescence staining for  $\gamma$ H2AX (magenta) and SENP6 (green) after 1 h, n=173 cells across 3 experiments. Middle and bottom panel: U2OS stably expressing wildtype GFP-SENP6 (GFP-SENP6<sub>WT</sub>) and a catalytic dead GFP-SENP6 (GFP-SENP6<sub>CD</sub>) were treated with IR and analyzed by immunofluorescence staining for  $\gamma$ H2AX (magenta) and GFP (green) after 1 h, n(GFP-SENP6<sub>WT</sub>)=148 and n(GFP-SENP6<sub>CD</sub>)=121 cells across 3 experiments. Representative images are shown. **a,c,f** Scale bar: 10  $\mu$ m.

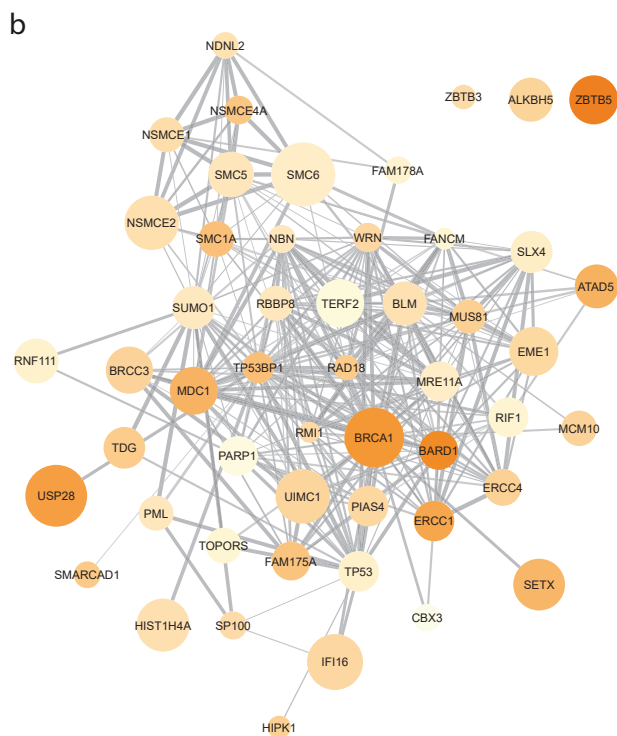


**Supplementary Fig 2. SENP6 does not localize to IR-induced DNA damage foci.** Top left panel: U2OS were treated with ionizing radiation (IR) and analyzed by immunofluorescence staining for  $\gamma$ H2AX (magenta) and SENP6 (green) at the indicated timepoints. n(10 min)=98, n(1 h)=81, n(4 h)=95 cells. Middle and bottom left panel: U2OS cells stably expressing wildtype GFP-SENP6 (GFP-SENP6<sub>WT</sub>) and a catalytic dead GFP-SENP6 (GFP-SENP6<sub>CD</sub>) were treated with IR and analyzed by immunofluorescence staining for  $\gamma$ H2AX (magenta) and GFP (green) at the indicated timepoints. n(10 min)=71, n(1 h)=82, n(4 h)=68 cells and n(10 min)=56, n(1 h)=48, n(4 h)=50 cells, respectively. Right panel shows the same experimental set-up as in the left panel, but a pre-extraction step was included before fixing the cells for immunofluorescence staining. n(10 min)=100, n(1 h)=104, n(4 h)=81 cells; n(10 min)=59, n(1 h)=70, n(4 h)=42 cells and n(10 min)=46, n(1 h)=48, n(4 h)=56 cells, respectively. Representative images are shown. Scale bar: 10  $\mu$ m.

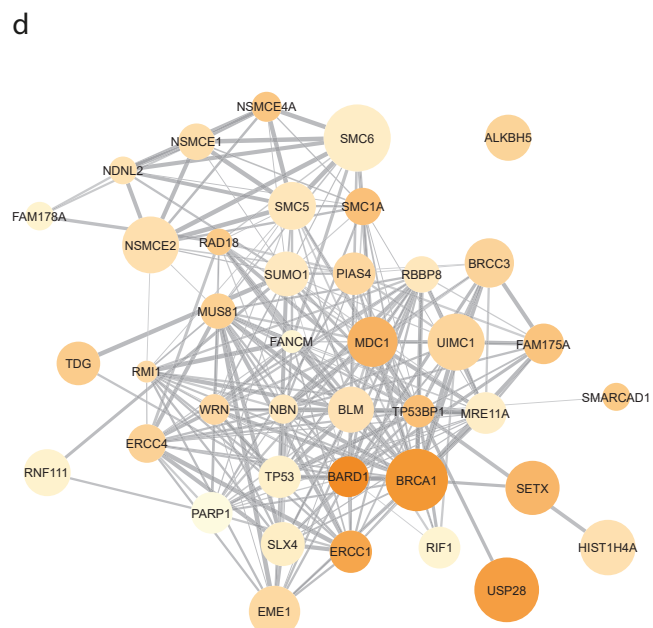




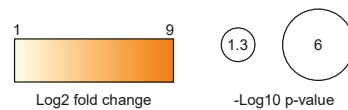
GO process: Double-strand break repair



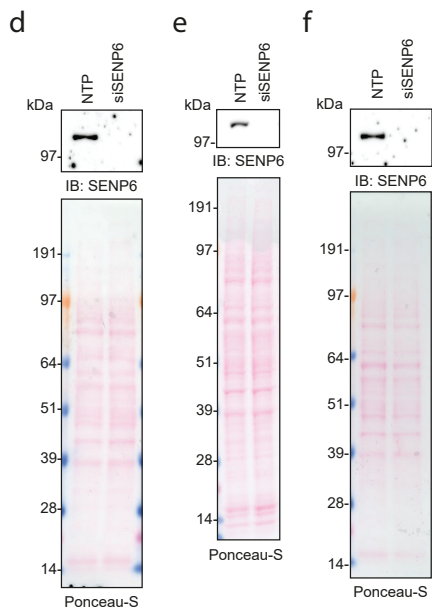
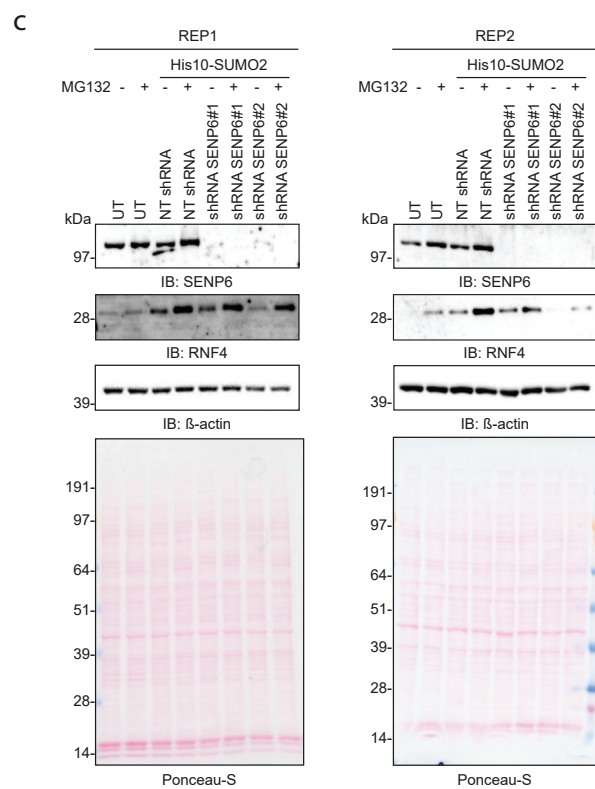
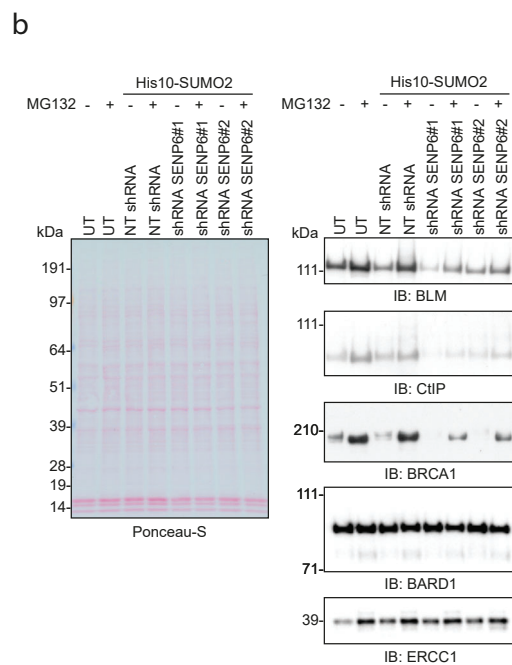
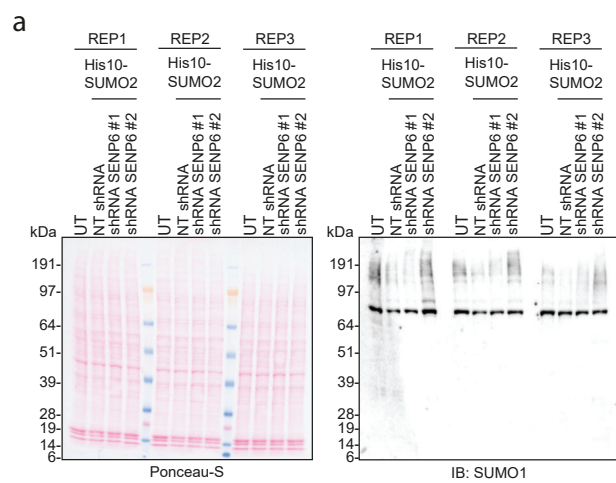
GO process: Cellular response to DNA damage stimulus



GO process: DNA repair

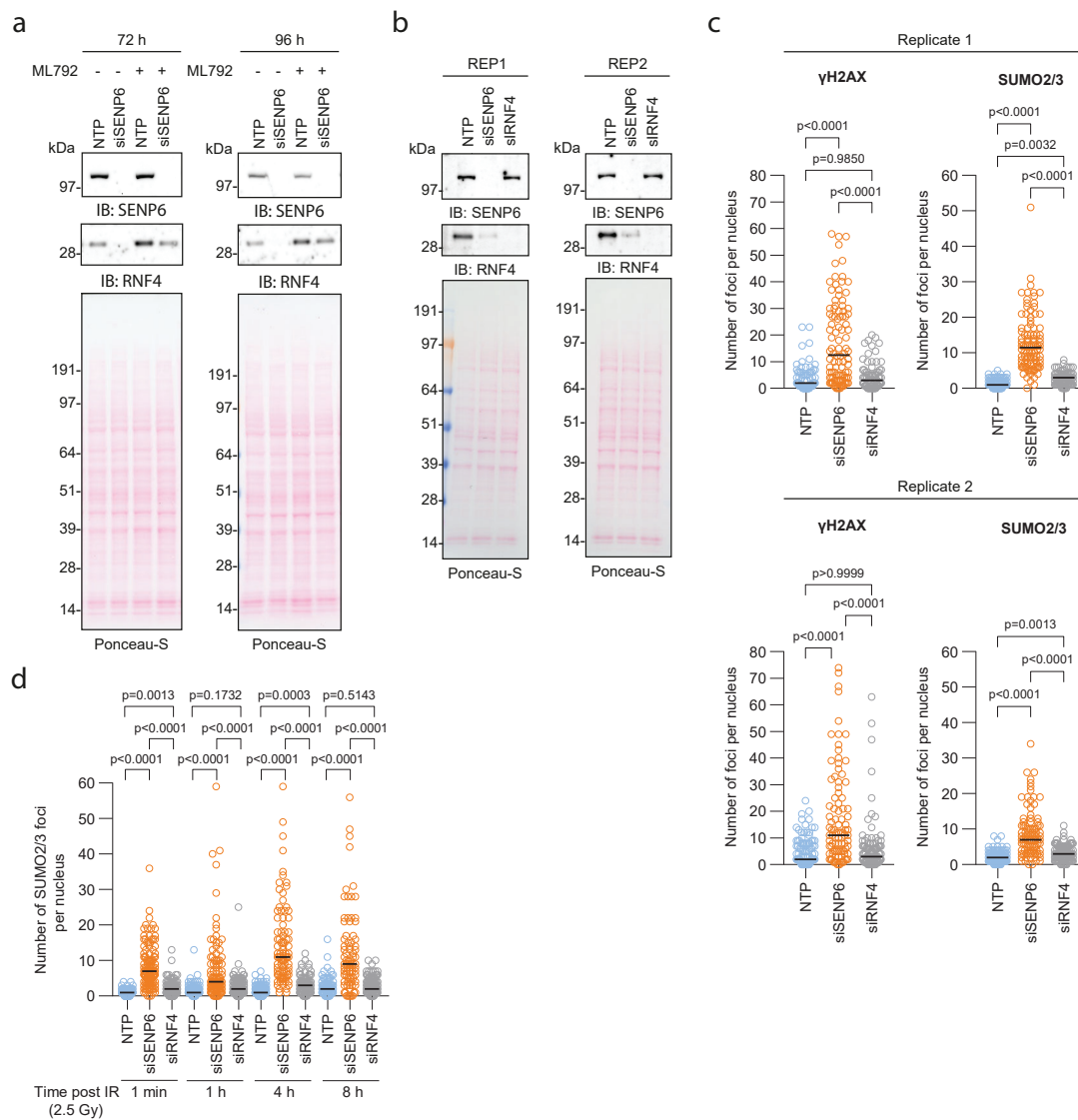


**Supplementary Fig 3. Identification of SENP6 targets by mass-spectrometry.** **a** Gene ontology (GO) enrichment analysis on the 180 SENP6 targets showing a significant increase in SUMO2 conjugation after SENP6 knockdown (Source proteomics data: ProteomeXchange Consortium via the PRIDE partner repository PXD011963). The enrichment ( $-\log$  FDR) and the number of genes (# genes) of the top GO processes involving the DNA damage response are plotted. **b-d** Protein STRING networks of the top GO processes involving the DNA damage response shown in **(a)**. The size of the nodes represents the  $-\log_{10}$  p-value and the color of the nodes the  $\log_2$  fold change of the enriched proteins after SENP6 knockdown compared with the nontargeting control. Size and color grading is indicated by the legend included in **(d)**. The width of the edges connecting the nodes represents the string score for protein-protein interactions curated from experimental data.

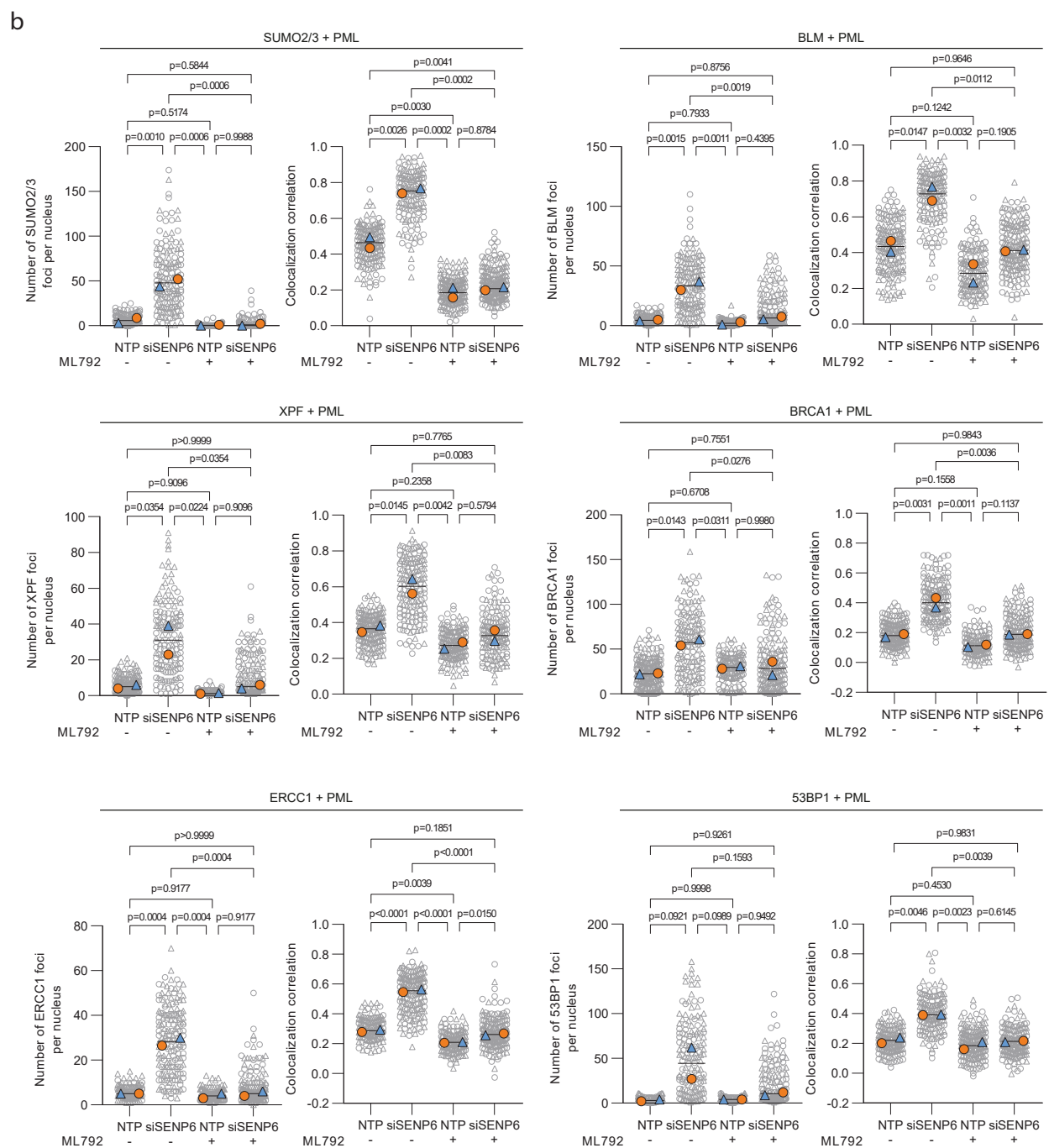
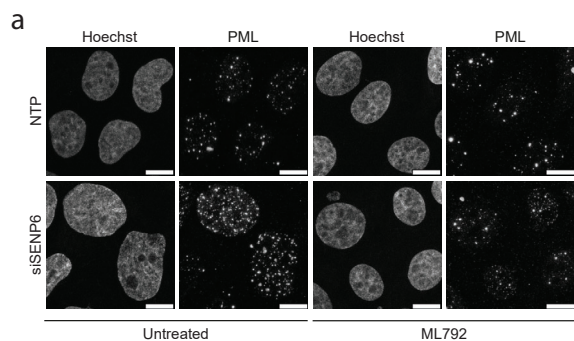




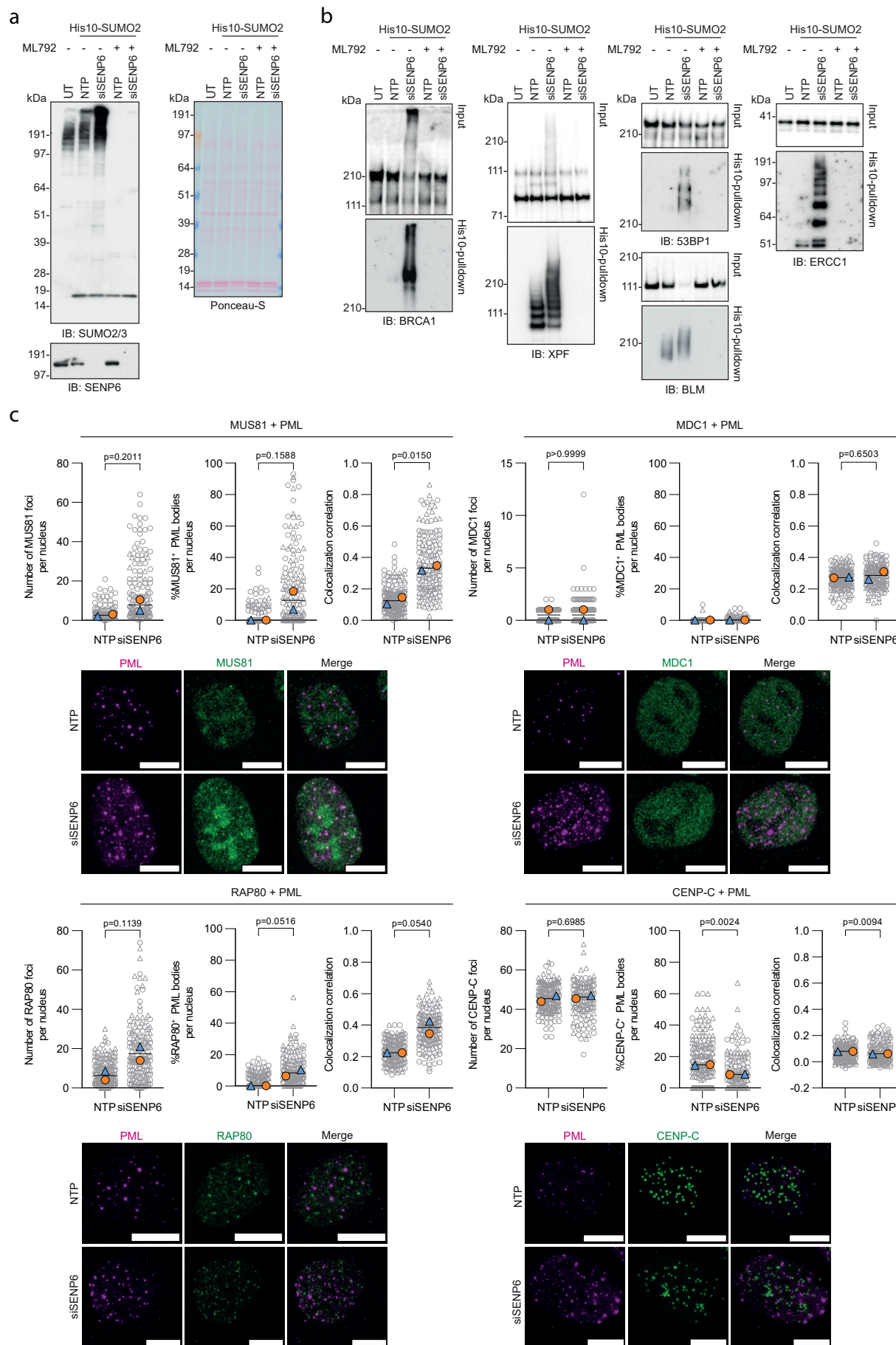
**Supplementary Fig 4. Potential role for SENP6 in regulation of DDR protein turnover.** **a** U2OS stably expressing His10-SUMO2 were infected with lentiviruses encoding shRNAs against SENP6 (shRNA SENP6#1 and #2) or a nontargeting control shRNA (NT shRNA). Cells were lysed three days post infection and analyzed by immunoblotting for SUMO1, n=3. Equal loading was verified by Ponceau-S staining. **b** U2OS stably expressing His10-SUMO2 were infected with lentiviruses encoding shRNAs against SENP6 (shRNA SENP6#1 and #2) or a nontargeting control shRNA (NT shRNA) and lysed three days post infection. Where indicated, cells were treated with 10  $\mu$ M MG132 for 6-8 h prior to lysis. Total lysates were immunoblotted for the indicated DDR proteins, n=2. Equal loading was verified by Ponceau-S staining. Representative blots are shown. **c** Lysates in **(b)** were also analyzed by immunoblotting for SENP6 and RNF4, n=2. Equal loading was verified by  $\beta$ -actin and Ponceau-S staining. **d** Immunoblot for SENP6, corresponding to Fig. 6a. Equal loading was verified by Ponceau-S staining. **e** Immunoblot for SENP6, corresponding to Fig. 6b. Equal loading was verified by Ponceau-S staining. **f** Immunoblot for SENP6, corresponding to Fig. 6c-h. Equal loading was verified by Ponceau-S staining.



**Supplementary Fig 5. Genomic instability after SENP6 depletion is not indirectly caused by RNF4 depletion.** **a** Lysates from cells corresponding to Fig. 1b-e and supplementary Fig. 1a-b (left panel) and Fig. 7c-d (right panel) were immunoblotted for SENP6 and RNF4, n=3. Equal loading was verified by Ponceau-S staining. Representative blots are shown. **b** U2OS were treated with SENP6 siRNAs (siSENP6), RNF4 siRNA (siRNF4) or nontargeting siRNAs (NTP) for 72 h and analyzed by immunoblotting for SENP6 and RNF4, n=2. Equal loading was verified by Ponceau-S staining. **c** NTP, siSENP6 and siRNF4 cells in **b** were analyzed by immunofluorescence staining for  $\gamma$ H2AX and SUMO2/3, n=2. Number of  $\gamma$ H2AX and SUMO2/3 foci per nucleus were quantified. Each datapoint represents a single cell (from left, n(1)=86,100,84 and n(2)=105,93,106 cells). Lines represent median. **d** U2OS were treated with siSENP6, siRNF4 or NTP siRNA for 72 h, treated with ionizing radiation (IR) and analyzed by immunofluorescence staining for  $\gamma$ H2AX and SUMO2/3 at the indicated timepoints. Number of SUMO2/3 foci per nucleus was quantified. Each datapoint represents a single cell (from left, n=103,77,103,82,119,95,88,80,116,103,96,107 cells). Lines represent the median. Significance was determined by two-sided one-way ANOVA with Dunnett's multiple comparison test at each timepoint.



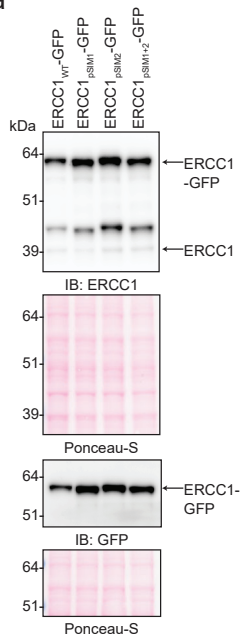
**Supplementary Fig 6. PolySUMOylated DDR proteins accumulate and localize to PML bodies. a** Microscopy images corresponding to Fig. 7c. U2OS were treated with SENP6 siRNAs (siSENP6) or nontargeting siRNAs (NTP) for 96 h and treated with or without 1  $\mu$ M ML792 for 24 h, n=6. Cells were analyzed by immunofluorescence staining for PML. Representative images are shown. Scale bar: 10  $\mu$ m. **b** Quantification corresponding to Fig. 7d for SUMO2/3 or DDR foci and PML bodies. The left graph shows the number of SUMO2/3 or DDR foci per nucleus. In the right graph colocalization of SUMO2/3 or DDR protein with PML bodies is estimated by Pearson correlation. Data are shown as pooled cells (grey), superimposed by the median percentage or correlation per experiment (blue and orange). Independent experiments are visualized by unique symbols. Lines represent the mean. Significance was determined by two-sided one-way ANOVA with Tukey's multiple comparison test.



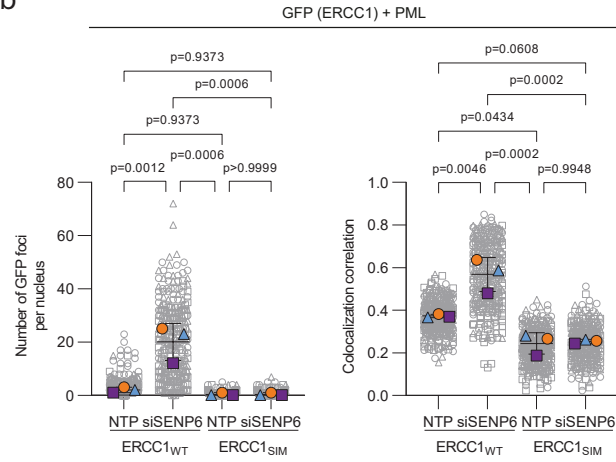


**Supplementary Fig 7. SUMO2/3 polymerization of proteins is required but not sufficient for PML body localization.** Total lysates corresponding to Fig. 7b were also immunoblotted for SENP6 and SUMO2/3 **(a)** and the indicated DDR proteins **(b)**, n=2. Same loading was used and verified by Ponceau-S staining. Representative blots are shown. **c** Cells corresponding to Fig. 7c-d were also stained for PML (magenta), and MUS81, RAP80, MDC1 or CENP-C (green). Left graph: number of DDR foci per nucleus; middle graph: colocalization quantified as percentage of PML bodies that colocalize with a DDR protein per nucleus; right graph: colocalization estimated by Pearson correlation. Data are shown as pooled cells (MUS81 from left, n=208,147; RAP80 from left, n=184,162; MDC1 from left, n=185,166; CENP-C from left, n=195,141 cells) (grey), superimposed by the median per experiment (blue and orange). Independent experiments are visualized by unique symbols. Lines represent the mean. Significance was determined with a two-sided unpaired t-test. For microscopy inserts, representative images of cells are shown. Scale bar: 10  $\mu$ m.

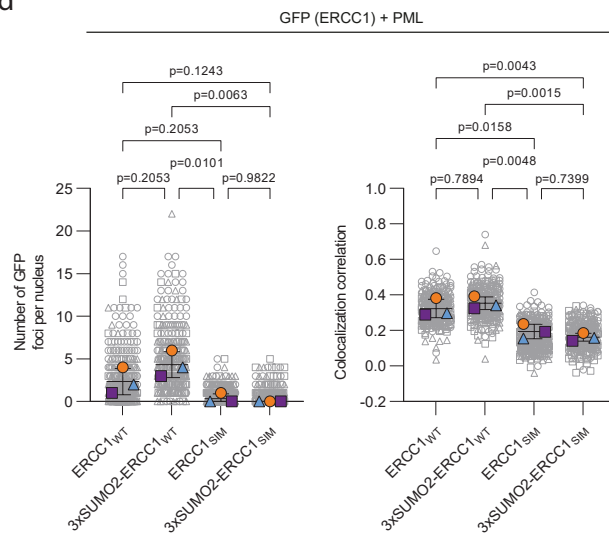
a



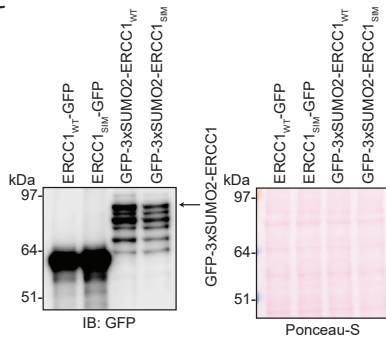
b



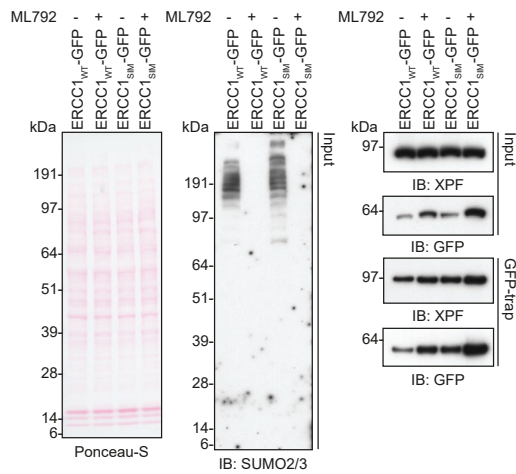
d



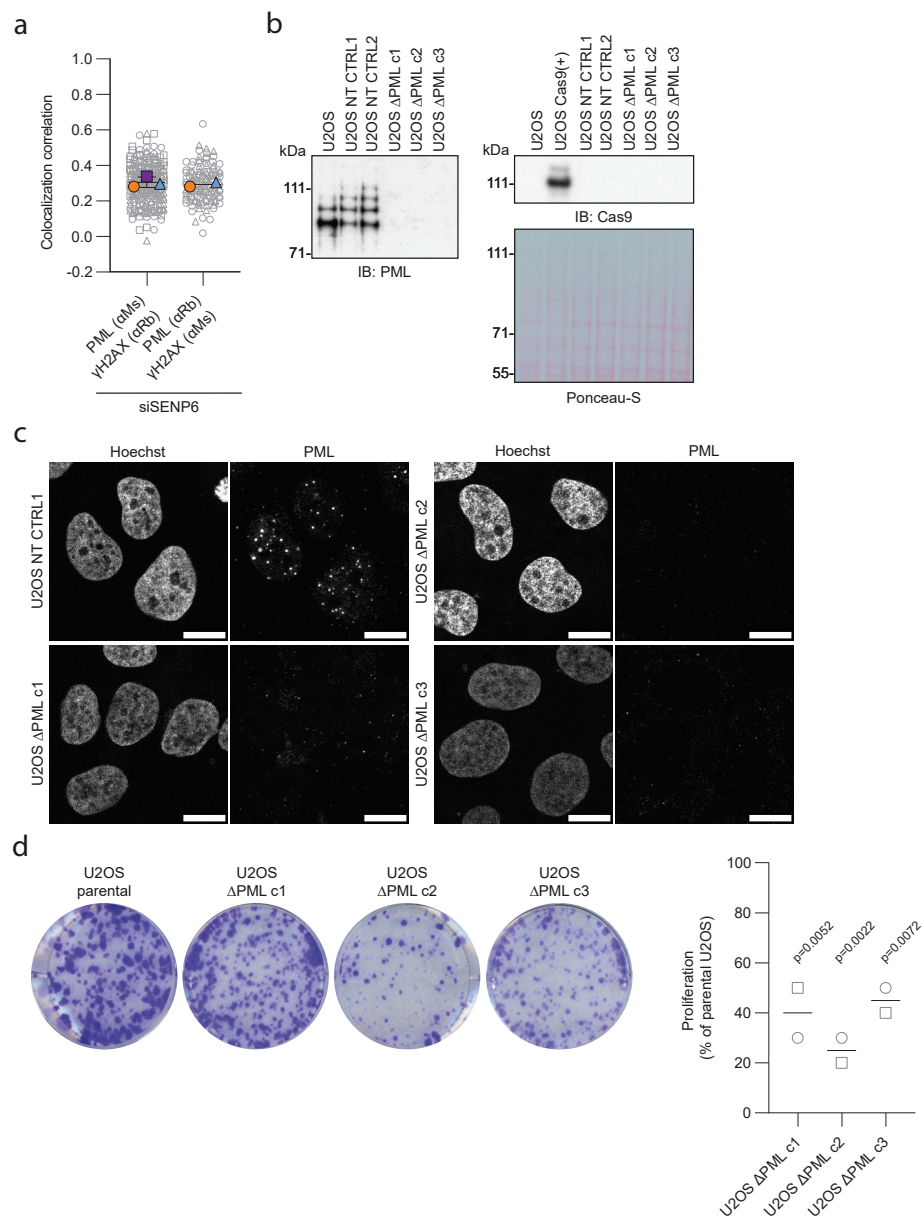
c



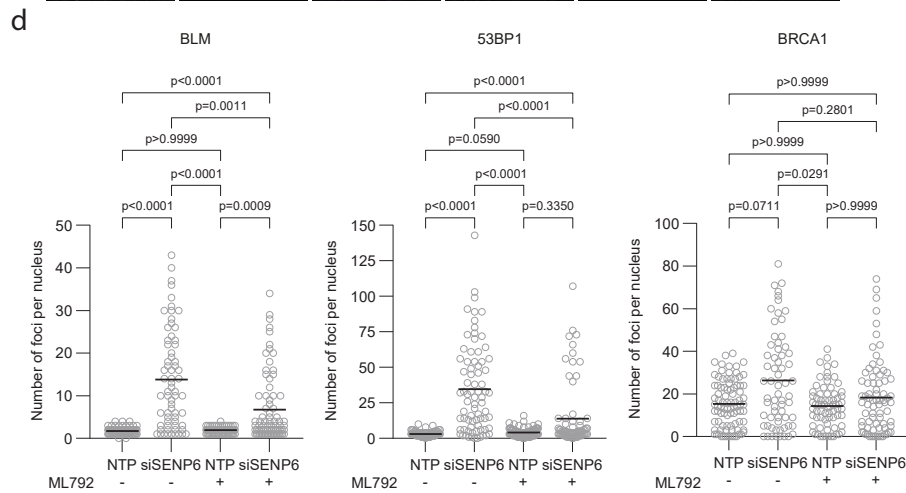
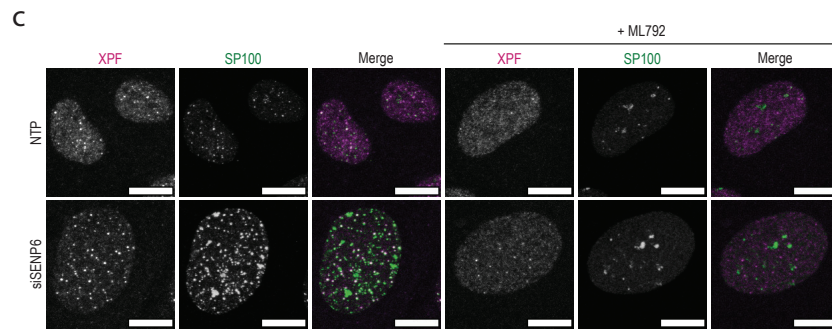
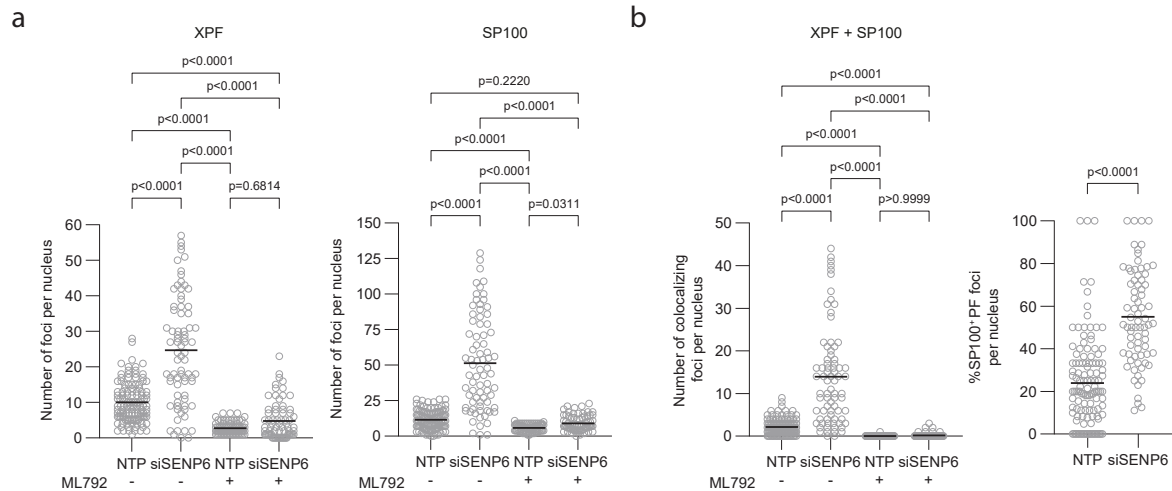
e



**Supplementary Fig 8. A functional SIM domain is required for ERCC1 accumulation and localization to PML bodies.** **a** U2OS stably expressing ERCC1-GFP or ERCC1-GFP with pSIM1, pSIM2 or both mutated were analyzed by immunoblotting for ERCC1 and GFP, n=3. Equal loading was confirmed with Ponceau-S staining. Representative blots are shown. **b** Quantification corresponding to Fig. 8d. The left graph shows the number of GFP foci per nucleus. In the right graph colocalization of GFP with PML bodies is estimated by Pearson correlation. **c** U2OS stably expressing GFP-3xSUMO2-ERCC1<sub>WT</sub> and GFP-3xSUMO2-ERCC1<sub>SIM</sub>, were immunoblotted for GFP, n=1. Equal loading was confirmed with Ponceau-S staining. **d** Quantification corresponding to Fig. 8e. The left graph shows the number of GFP foci per nucleus. In the right graph colocalization of GFP with PML bodies is estimated by Pearson correlation. **b,d** Data are shown as pooled cells (grey), superimposed by the median per experiment (blue, orange and purple). Independent experiments are visualized by unique symbols. Error bars represent mean  $\pm$ SD. Significance was determined by two-sided one-way ANOVA with Tukey's multiple comparison test. **e** Western blot images corresponding to Fig. 8f. U2OS stably expressing ERCC1-GFP wildtype (ERCC1<sub>WT</sub>-GFP) or ERCC1-GFP SIM mutant (ERCC1<sub>SIM</sub>-GFP) were treated with or without 1  $\mu$ M ML792 for 24 h. ERCC1<sub>WT/SIM</sub>-GFP were purified and samples were analyzed by immunoblotting for GFP and XPF. Equal loading of lysates was verified by Ponceau-S staining. Representative blots are shown.



**Supplementary Fig 9. PML is not causally involved in the genomic instability induced by SENP6 knockdown.** **a** Quantification corresponding to Fig. 9a.  $\gamma$ H2AX and PML colocalization was estimated by Pearson correlation. Data are shown as pooled cells (from left,  $n=232,125$  cells) (grey), superimposed by the median correlation per experiment (blue, orange and purple). Data is shown for siSENP6-treated cells from  $n=3$  for  $\alpha$ -PML mouse (Ms) and  $\alpha$ - $\gamma$ H2AX rabbit (Rb), and  $n=2$  for  $\alpha$ -PML Rb and  $\alpha$ - $\gamma$ H2AX Ms costaining. Error bars represent mean  $\pm$ SD. **b** Cell lysates from U2OS and U2OS  $\Delta$ PML cells (c1, c2, c3) were immunoblotted for PML and Cas9 to confirm knockout of PML and no stable integration of GFP-Cas9. U2OS transiently transfected with the GFP-Cas9-expressing plasmid were included as positive control for Cas9 immunoblotting. Two clones from U2OS transfected with a non-targeting gRNA (NT CTRL1 and NT CTRL2) are shown as additional control cell lines. Equal loading was verified by Ponceau-S staining. **c** U2OS  $\Delta$ PML cells (c1, c2, c3) were analyzed by immunofluorescence staining for PML. A clone from U2OS transfected with a non-targeting gRNA (NT CTRL1) is shown as additional control cell line. Representative images are shown. Scale bar: 10  $\mu$ m. **d** Colony forming assay of U2OS and U2OS  $\Delta$ PML cells. Cells were seeded at the same density and fixed and stained with crystal violet after 14 days,  $n=2$ . Representative images (left) and quantification of solubilized crystal violet (right) are shown. Independent experiments are visualized by unique symbols. Cell proliferation is shown as percentage, with parental U2OS set at 100% proliferation. Significance between U2OS  $\Delta$ PML cells and parental U2OS was determined by two-sided one-way ANOVA with Dunnett's multiple comparison test.





**Supplementary Fig 10. Accumulation of DDR proteins in condensates after SENP6 depletion can occur independently of PML. a** U2OS were treated with SENP6 siRNAs (siSENP6) or nontargeting siRNAs (NTP) for 96 h and treated with or without 1  $\mu$ M ML792 for 24 h. Cells were analyzed by immunofluorescence staining for XPF (magenta) and SP100 (green). Number of XPF (left panel) and SP100 (right panel) foci per nucleus was quantified. Significance was determined by two-sided one-way ANOVA with Dunnett's multiple comparison test. **b** Number of XPF and SP100 colocalizing foci per nucleus was quantified (left panel). Significance was determined by two-sided one-way ANOVA with Dunnett's multiple comparison test. Percentage of SP100<sup>+</sup> XPF foci per nucleus was quantified (right panel). Significance was determined with a two-sided Mann-Whitney U test. **a,b** From left, n=121,76,78,73 cells. **c** Representative microscopy images corresponding to **(a-b)**. Scale bar: 10  $\mu$ M. **d** Cells in **(a-c)** were also stained for BLM (left panel), 53BP1 (middle panel) and BRCA1 (right panel). Number of foci per nucleus was quantified. From left, n(BLM)=92,66,89,78; n(53BP1)=95,76,96,75; n(BRCA1)=89,65,72,76 cells. Significance was determined by one-way ANOVA with Dunnett's multiple comparison test. **a,b,d** Lines represent the median.

**Supplementary Table 1. Key resources**

Reagent or resource	Source	Identifier
<b>Antibodies</b>		
anti-SEN6 (IB <sup>a</sup> 1:100; IF <sup>b</sup> 1:50)	Sigma-Aldrich	WHP0026054M1
anti-SEN7 (IB 1:1000)	Bethyl	A302-995A
anti-SUMO2/3 8A2 (IB 1:250)	University of Iowa	8A2
anti-SUMO2/3 2277 (IF 1:100)	Eurogentec	<sup>1</sup>
anti-SUMO1 2C7 (IB 1:1000; IF 1:100)	Zymed laboratories Inc.	18-2306
anti-PML (IB 1:100; IF 1:500)	Bethyl	A301-167A
anti-PML (IB 1:1000; IF 1:1000)	MBL	M041-3
anti-γH2AX (IB 1:500; IF 1:500)	Merck Millipore	05-636
anti-γH2AX (IB: 1:500)	Cell signaling technology	9718
anti-RNF4 (IB 1:3000)	Eurogentec	<sup>2</sup>
anti-ERCC1 (IF 1:100)	Abcam	ab129267
anti-ERCC1 (IB 1:500-1:1000)	Cell signaling technology	12345
anti-BLM (IB 1:1000; IF 1:200)	Abcam	ab2179
anti-XPF (IB 1:500)	Thermo Fisher Scientific	MS-1381
anti-XPF (IF 1:100)	Santa Cruz	sc-136153
anti-MUS81 (IB 1:500-1:1000; IF 1:250)	ImmuQuest	IQ285
anti-53BP1 (IB 1:1000; IF 1:500)	Bethyl	A300-272A
anti-BRCA1 (IB: 1:500)	Cell signaling technology	9010
anti-BRCA1 (IF 1:1000)	Merck Millipore	07-434
anti-RAP80 (IB 1:1000; IF 1:200)	Bethyl	A300-763A
anti-MDC1 (IB 1:1000; IF 1:500)	Bethyl	A300-052A
anti-CtIP (IB 1:1000; IF 1:200)	Bethyl	A300-488A
anti-EME1 (IB 1:1000)	ImmuQuest	IQ284
anti-BARD1 (IB 1:1000)	Bethyl	A300-263A
anti-Sp100 (IB 1:1000)	Chemicon international	AB1380
anti-RAD51 (IB 1:500)	Cell signaling technology	8875
anti-Ubiquitinated proteins FK2 (IB 1:1000)	Merck Millipore	04-263
anti-CENP-C (IF 1:100)	Merck Millipore	MABE1114
anti-GFP (IB 1:5000; IF 1:500)	Novus Biololgicals	NB600-308
anti-Cas9 (IB 1:1000)	Cell Signaling technology	14697
Alexa-Fluor 568 goat-anti-rabbit / goat-anti-mouse (IF 1:250)	Invitrogen	A11004 / A11011
Alexa-Fluor 488 goat-anti-rabbit / goat-anti-mouse (IF 1:250)	Invitrogen	A11034 / A11001
<b>Oligonucleotides</b>		
SMART pool ON-TARGETplus SEN6 siRNA	Dharmacon	L-006044-00-00
ON-TARGETplus RNF4 siRNA	Dharmacon	J-006557-08
SMART pool ON-TARGET siRNA nontargeting	Dharmacon	D-001810-10-
shRNA SEN6 #1- GACAGAACTAACAGAAGAGAA	Sigma-Aldrich MISSION® shRNA library	TRC -004103
shRNA SEN6#2-CACAGGATTAACAACCAAGAA	Sigma-Aldrich MISSION® shRNA library	TRC-004104
Non-targeting shRNA	Sigma-Aldrich MISSION® shRNA library	TRC-SHC002
shRNA RNF4 #1- CATACTCCCAGAAACGCCAGG	Sigma-Aldrich MISSION® shRNA library	TRC-272668

shRNA RNF4 #2- CATACTCCCAGAAACGCCAGG	Sigma-Aldrich MISSION® shRNA library	TRC-284821
ERCC1 pSIM1 FWD: 5'- GCCAGCAAGGAAGAAATTTGCGGCACCCGCCG ACGAGGATGAGGTCCCTC-3'	This study, to generate ERCC1 <sub>pSIM1</sub>	N/A
ERCC1 pSIM1 REV: 5'- GAGGGACCTCATCCTCGTCGGCGGGTGCCGCAA ATTTCTTCTTGCTGGC-3'	This study, to generate ERCC1 <sub>pSIM1</sub>	N/A
ERCC1 pSIM2 FWD: 5'- CCGGGGCAAATCCAACAGCGCCGCTGCGAGC CCTCGGCAGAGGGGCA-3'	This study, to generate ERCC1 <sub>pSIM2</sub>	N/A
ERCC1 pSIM2 REV: 5'- TGCCCTCTGCCGAGGGCTCGCAGCGGCGCTGT TGGATTTGCCCGG-3'	This study, to generate ERCC1 <sub>pSIM2</sub>	N/A
ERCC1 EcoRI 5': 5'- taagcagaattcATGGACCTGGGAAGGACAAAG- 3'	This study, to clone ERCC1 into pDONR207-3X-ΔN11-3X- SUMO2-ΔGG-CENPW	N/A
ERCC1 STOP NotI 3': 5'- tgcttagcgccgcTCAGGGTACTTCAAGAAGGG- 3'	This study, to clone ERCC1 into pDONR207-3X-ΔN11-3X- SUMO2-ΔGG-CENPW	N/A
<b>Recombinant DNA</b>		
pSpCas9(BB)-2A-GFP (PX458)	Addgene	48138
pDONR223-ERCC1 ORF	Sigma-Aldrich MISSION® TRC3 Human ORF Collection	Legacy clone name: ORF001395.1_s300c1
pU6-gRNA/PGK-Puro-2A-BFP with gRNA sequence: 5'- ATCCAAGAAAGCCAGCCCAGAGG-3'	Sigma-Aldrich Human Sanger Arrayed Whole Genome Lentiviral CRISPR library	Clone ID: 226656931
pBABE-puro-ERCC1 <sub>WT</sub> -GFP	This study	N/A
pBABE-puro-ERCC1 <sub>pSIM1</sub> -GFP	This study	N/A
pBABE-puro-ERCC1 <sub>pSIM2</sub> -GFP	This study	N/A
pBABE-puro-ERCC1 <sub>pSIM1+2</sub> -GFP	This study	N/A
pBABE-puro-GFP-3xSUMO2-ERCC1 <sub>WT</sub>	This study	N/A
pBABE-puro-GFP-3xSUMO2-ERCC1 <sub>SIM</sub>	This study	N/A
pCW57.1-GFP-SENp6 <sub>WT</sub> -kd-resistant	<sup>3</sup>	N/A
pCW57.1-GFP-SENp6 <sub>CD</sub> -kd-resistant	<sup>3</sup>	N/A
pHis-TEV30a-His10-ΔN11-SUMO2-trimer	<sup>4</sup>	N/A
pDONR207-3X-ΔN11-3X-SUMO2-ΔGG-CENPW	This study	N/A

<sup>a</sup>IB: immunoblotting; <sup>b</sup>IF: immunofluorescence

## References

- 1 Vertegaal, A. C. O. *et al.* A Proteomic Study of SUMO-2 Target Proteins. *J of Biol Chem* **279**, 33791-33798 (2004).
- 2 Vyas, R. *et al.* RNF4 is required for DNA double-strand break repair in vivo. *Cell Death & Differentiation* **20**, 490-502 (2013).
- 3 Liebelt, F. *et al.* The poly-SUMO2/3 protease SENP6 enables assembly of the constitutive centromere-associated network by group deSUMOylation. *Nat Commun* **10**, 3987 (2019).
- 4 Eifler, K. *et al.* SUMO targets the APC/C to regulate transition from metaphase to anaphase. *Nat Commun* **9**, 1119 (2018).